Test Results of the 36 T, 1 ppm Series-Connected Hybrid Magnet System at the NHMFL

Mark. D. Bird, *Senior Member, IEEE*, Hongyu Bai, Iain R. Dixon, *Member, IEEE*, and Andrew V. Gavrilin

***Abstract*—The National High Magnetic Field Laboratory (NHMFL) has completed testing and commissioning of a unique ultrahigh field magnet that provides 36 T in a 32 mm bore with field inhomogeneity and stability better than 1 ppm over a cylinder of 1 cm diameter and length and a duration up to a few hours. While the magnet meets all its primary performance goals, there were some unexpected observations during the testing and commissioning activities. Primarily, while the magnet reaches full current and field, we are unable to charge the magnet as quickly as was anticipated. Also, the magnet occasionally quenches for no apparent reason. Charging the magnet at slower rates reduces the probability of quenches.**

***Index Terms*—Cable-in-conduit magnet, high field magnet, hybrid magnet, resistive magnet.**

I. Introduction

THE NHMFL develops and operates high field magnets in seven user facilities in Tallahassee and Gainesville, Florida and Los Alamos, New Mexico. The DC Field facility in Tallahassee is at Florida State University (FSU) and includes resistive magnets providing up to 41.5 T and resistive/superconducting hybrid magnets providing up to 45 T. While approximately 20 hybrid magnets have been installed worldwide, all the previous ones were mainly used for Condensed Matter Physics (CMP) at high fields [1]. For a typical high field magnet, either resistive or hybrid, the homogeneity is 200 – 500 ppm over a 1 cm spherical volume and stability is typically 50 ppm/min or worse [2] due to the 10 – 30 MW of power required.

In recent years the NHMFL developed a new series-connected hybrid magnet providing a world-unique magnet of 36 T in a 40 mm bore with inhomogeneity $<$ 1 ppm/cm and instability $<$ 0.1 ppm/min to be used for solid-state NMR [3], [4]. The improved stability was provided by connecting the resistive and superconducting magnets electrically in series. The relatively high inductance of the superconducting coil (0.25 H) results in a ten-fold reduction in field ripple in this Series-Connected Hybrid (SCH) compared with typical resistive magnets (5 mH) operating on the same power supply. In addition, an NMR lock was used to reduce the ripple to $\sim$0.1 ppm over 3 minutes [4]. To reach the high homogeneity level, current-density grading was used in the coils of the resistive magnet which allowed us to reach $\sim$50 ppm/cm. Ferromagnetic and resistive shims in the bore of the magnet allowed us to reach $<$1 ppm/cm [4].

Another unusual feature of this magnet was that it was developed as one of a set of two hybrids built using the same Nb_3Sn Cable-in-Conduit Conductors (CICC) and CICC coils. The other magnet was developed for the Helmholtz Zentrum Berlin (HZB) using a copy of the superconducting coil, and a 4 MW resistive magnet. The entire HZB system was mounted with a horizontal bore and is used for neutron scattering [5], [6]. It provides up to 26 T and was first tested in 2014 and operated with neutron scattering in 2015. A third similar CICC magnet for Radboud University in Nijmegen (RUN), The Netherlands, was later added to the series. Its CICC coil uses the same conductors but has a slightly larger inner diameter and length. This coil was designed jointly by the two labs, fabricated at FSU, and has been delivered to RUN [7].

The superconducting parts of the three hybrids consist of three grades of conductor: High-Field (HF), Mid-Field (MF) and Low-Field (LF). The three grades have similar amounts of Cu, but the amount of Nb_3Sn is highest in the HF and least in the LF. Each is a solenoid consisting of 18 nested layers: 3 of HF, 3 of MF, and 12 of LF. The superconducting coils of the HZB and FSU magnets provide 13 T on the axis at the mid-plane of the magnet while the RUN version should provide 12.3 T.

II. CICC Temperature Margin

A. Design Goals and Process

FSU's SCH was intended not only for solid-state NMR but also for traditional CMP which routinely, unlike NMR, requires collecting data as a function of field. Consequently, one of the design goals was to be able to continuously energize and de-energize (ramp) the magnet at 36 A/s (9.2 minutes from zero to full field for this 20-kA magnet). The HZB magnet used the same design for the Nb_3Sn coil, but was only intended to ramp at 12 A/s (27.7 minutes from zero to full field). The conductors were extensively tested to find the critical surface and AC losses associated with energizing [8], [9] and the data was fit with the Twente critical current function [10]. The final Twente fit parameters are listed in Table I. Effective strain and critical current, I_c, degradation values are shown in Table II. The HF CICC was tested at the SULTAN facility which cannot apply

Manuscript received October 30, 2018; accepted January 16, 2019. Date of publication January 25, 2019; date of current version February 11, 2019. This work was supported by the National High Magnetic Field Laboratory which is supported by National Science Foundation Cooperative Agreement DMR-1644779 and the State of Florida. *(Corresponding author: Mark D. Bird.)*

The authors are with the National High Magnetic Laboratory, Florida State University, Tallahassee, FL 32310 USA (e-mail: bird@magnet.fsu.edu; bai@magnet.fsu.edu; idixon@magnet.fsu.edu; gavrilin@magnet.fsu.edu).

Color versions of one or more of the figures in this paper are available online at http://ieeexplore.ieee.org.

Digital Object Identifier 10.1109/TASC.2019.2895569

TABLE I
TWENTE FIT PARAMETERS FROM CICC TESTING

Parameter	Value	Units
C_{a1}	114.14	
C_{a2}	82.75	
$\varepsilon_{0,a}$	0.237	%
ε_m	-0.11	%
B_{c2m}* (0)	29.05	T
T_{cm}* (0)	15.91	K
C_1	49,040	A * T

The Twente critical current function is defined in [10].

TABLE II
INTERPRETATION OF CIC TEST CONDUCTORS

Conductor	Effective Strain (%)	*Measured I_c* Degradation (%)	*Design I_c Degradation (%)*
HF	-0.65	0	13
MF standard	-0.65	16	25
MF alternate	-0.72	0	0
LF	-0.75	0	10

tension to the conductors. The effective strain in the HF strand was determined directly from the I_c and T_{cs} data. The MF and LF CICCs were tested at FSU's facility which can apply tension. For these conductors, the "standard" interpretation of the data was to set the effective strain to that where the maximum T_{cs} was found. An additional I_c degradation was then used to match the measured data. An "alternative" interpretation chooses the strand strain to match the performance with no degradation (the same as for the HF where tension could not be applied). For design of the magnets we assumed there would be additional I_c degradation compared with what was measured in the tests, as shown in the last column of Table II. We see that measured effective strain in the CICCs varied between 0.65% and 0.75%. This is consistent with other CICCs measured worldwide, but much less than the 0.92% difference between Nb_3Sn and stainless steel during cool-down from reaction temperature (640 °C) to operating temperature (4 K) [11].

AC losses were measured only for the HF conductor and only in one direction, parallel to the long dimension of the CICC. The coupling loss time constant $n\tau$, was determined as a function of frequency. This one value was used for both the parallel and transverse directions in all three conductors during the design phase.

Temperature margins during operation were predicted using GANDALF with in-house major modifications [12]. The calculations indicated that we should be able to continuously and safely ramp the FSU SCH up and down at 36 A/s and that the minimum temperature margin in the outsert would be about 1.5 K (Fig. 1) at the steady-state mass flow rate of supercritical helium (SHe) of 10 g/s. The heating due to AC losses (both hysteresis and coupling) is a maximum at low field. Consequently, the minimum temperature margin occurs at the top of the second cycle (Fig. 1).

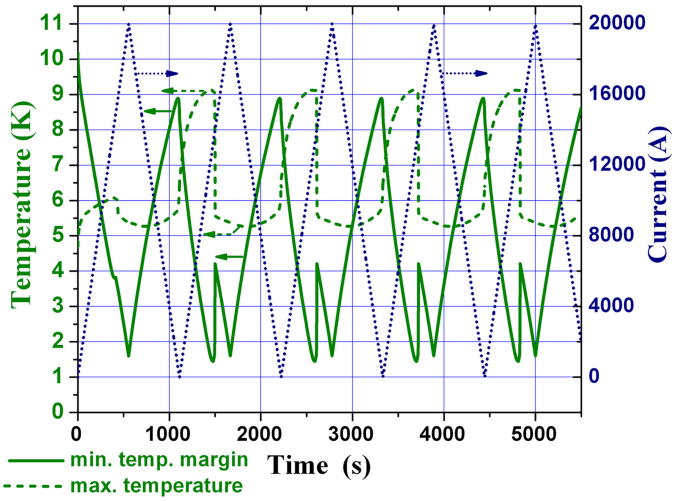

Fig. 1. Current, CICC maximum temperature, and minimum temperature margin vs time for the innermost layer of the HF conductor computed by our GANDALF-based code at 36 A/s and 10 g/s using the low ac losses measured on a test conductor at SULTAN.

TABLE III
INITIAL SCH CHARGING PROTOCOL AT HZB: OCT. 2014, 38.7 MIN

Ramp Rate (A/s)	Starting Current (kA)	Final Current (kA)	Duration (min)
15	0	9	10
0	9	9	2
10	9	18	15
0	18	18	2
5	18	20	6.7

Given that the field is a maximum at the inner diameter of a solenoid, and decreases monotonically outward through the coil, the innermost layers of the HF, MF, and LF conductors, i.e., layers 1, 4, and 7 were designed to have the smallest temperature margins, with the absolute minimum in layer 4. Consequently, if quenches were to occur, we would expect them to occur in one of those three layers.

The SHe flow rate through the magnet (10 g/s) corresponds to ~10.3 min to replace warm SHe in the inner layer of the magnet with new, cold SHe. This is a slightly longer time than we expected to take to ramp the magnet (9.5 min).

B. HZB Testing Experience

All testing of the CICC coils at HZB and FSU was carried out with the resistive coil electrically in series with the CICC coil and power supplies. The power supplies were designed to operate on a resistive load and it is not practical to test the outsert by itself. When the first magnet was tested in Berlin in Oct. 2014, we were unable to charge the magnet at the 12 A we were expecting. Through trial and error we found a charging protocol (Table III) that was adopted for initial use at HZB.

A few months later the charging process was slowed even further before quenches were eliminated. The new process is shown in Table IV.

TABLE IV
FINAL SCH CHARGING PROTOCOL AT HZB: 2015, 55.5 MIN

Ramp Rate (A/s)	Starting Current (kA)	Final Current (kA)	Duration (min)
10	0	8	13.3
0	8	8	4
10	8	14	10
0	14	14	4
7	14	16	4.8
0	16	16	4
7	16	18	4.8
0	18	18	4
5	18	20	6.7

TABLE V
COUPLING LOSS TIME CONSTANTS FOR 20 KA CICCS

TYPE OF CICC	LOCATION	PARALLEL (SEC)	TRANSVERSE (SEC)	VOID FRACTION (%)
FSU HF TEST	SULTAN	0.175	?	28
FSU HF AS-BUILT	TWENTE	0.6	5.7	24
RUN HF TEST	TWENTE	0.06	1.5	25
RUN MF TEST	SULTAN	1.5	2.5	24

C. Nijmegen Data

In 2012 the NHMFL signed the agreement to work with RUN to develop a 45 T hybrid using Nb_3Sn CICCs very similar to those used for the HZB and FSU magnets. As part of that project, it was possible to perform new conductor tests.

The MF conductor was of interest because it was believed to have the smallest temperature margin and its AC losses had not been previously measured. Consequently, it was tested at SULTAN to determine both thermal strain and AC losses with results being available in 2015 [13]. Because the HZB magnet was by then reaching field, but not as quickly as we intended, due to quenches in the HF conductor, there was a suspicion that the AC losses in the HF conductor were higher than previously believed. Consequently, AC loss was (re-)measured at the University of Twente both for an "as-built" FSU CICC and a slightly different test CICC for the RUN project [14]. Results for the three HF AC loss measurements are in Table III. We see that the as-built HF CICC used for the FSU and HZB magnets had much higher AC loss than either the test conductors for FSU/HZB or Nijmegen. The variation was seen to be as large as a factor of ten. This variation might have been due to the different void fractions of the various conductors as show in the right column of Table V.

The new tests on the MF conductor provided I_c results very similar to those measured at FSU except the I_c degradation was 4% less (alternatively thermal compression 0.02% less). However, the AC losses were also significantly higher than had been assumed based on measurements of HF conductor.

D. FSU Testing Experience

In November 2016 we started testing the Tallahassee magnet and used the October 2014 HZB protocol with 10 g/s SHe flow which worked reliably. This charging procedure was more than 4 times slower than the rate we had expected to be able to charge the FSU magnet. This means the SHe should be replaced four times during ramping up.

After shimming and stabilizing the magnet, we started to serve users and simplified the protocol to allow the users to charge and discharge the magnet themselves as long as the rate was below a certain value (and the SHe flow rate was $\geq$10 g/s). Consequently the magnet was charged at a constant 8.6 A/s with no waiting at fixed current. (Both this and the Oct 2014 HZB protocol take 38.7 minutes to reach full field). There was only one quench in the first four months of nearly daily operations in 2017.

Because we had experienced only one quench and the users were eager to ramp more quickly, we decided to try to find the ramp-rate limit for the magnet. On May 11, 2017 we ramped the magnet up, down, up again at 9 A/s, then continued cycling, typically increasing the ramp rate at the start of a down ramp and maintaining that rate going down and back up. This was done because the minimum temperature margin occurs at 20 kA and is smaller the faster the ramp rate was during the previous low-current phase. We did not experience a quench until ramping up at 20 A/s when the magnet quenched at 16.3 kA. See Table VI.

TABLE VI
RAMPING PATTERN TO DETERMINE MAXIMUM ALLOWABLE RATE

Cycle	Ramp Rate (A/s)	Starting Current (kA)	Final Current (kA)
1	9	0	20
	9	20	0
2	9	0	20
	12	20	0
3	12	0	20
	14	20	0
4	14	0	20
	15	20	0
5	16	0	20
	18	20	0
6	18	0	20
	20	20	0
7	20	0	16.3

E. Operating Experience

Based on these results we thought the magnet could be reliably operated with 18 A/s ramp rate (at 10 g/s SHe flow rate) and it was returned to service with limits set appropriately. On the first cycle the magnet quenched at 16.0 kA. We then lowered the allowed ramp rate to 15 A/s and operated a few days until it quenched at 19 kA on May 18. The ramp rate was then reduced to 12 A/s which was used until June 20 when it quenched at 17 kA and the ramp rate was lowered further to 10 A/s. There were additional quenches on July 14 and Aug 31 and the SHe flow rate was increased from 10 g/s to 16 g/s.

In January 2018 the SHe flow rate was increased further to 18 g/s. Table VII presents data on most of the quenches experienced at FSU while Table VIII presents summary statistics for both FSU and HZB.for different ramp rates and flow rates.

TABLE VII
FSU QUENCH DATA WITH 10 G/S SHE FLOW

Date	1/12	5/11	5/12	5/18	6/20	7/14	8/31
Rate (A/s)	15	20	9	13	8	9	8
Current	18	16.3	16	19	17	18	18
Layer	2	3	1	1	2	2	2

TABLE VIII
QUENCH STATISTICS

Ramp Rate (A/s)	SHe Flow Rate (g/s)	# of Cycles	# of Quench	Quench/ Cycle (%)
12 – 18	10	33	5	15
10	10	31	2	6.4
10	16	79	2	2.5
10	18	58	0	<1.7
HZB -1 FSU	10	38	0	<2.6
HZB - 2 HZB	13	>120	0	<0.8
Overall	N/A	>359	9	2.5

"HZB-1 FSU" indicates the ramp rates were those indicated in Table III using the FSU magnet. "HZB-2 HZB" indicated that ramp rates indicated in Table IV using the HZB magnet.

We are not aware of other CICCs demonstrating unreliable ramp rates, however, this has been seen both in the HZB and FSU magnets.

While the designed temperature margins are smallest in layers 1, 4, and 7, quenches have actually occurred in layers 1, 2 and 3; all three HF layers and none in the MF or LF layers. This suggests the HF conductor is not meeting performance specifications.

F. Re-Assessment of Temperature Margins

Given that both HZB and FSU magnets would reach full current, but only if we charged ~6 times slower than planned, it appeared the AC losses in the magnets must be higher than the design values. AC losses in the magnet were measured by cycling the magnet at 5 A/s from 0.2 kA to 5 kA and back five times while measuring the inlet and oulet SHe flow rate, pressure and temperature. The average power was determined to be 70.9 W. This is 13% lower than computed based on the losses measured at Twente using real FSU CICC.

We re-ran the stability calculations based on the measured AC losses. With SHe flow of 10 g/s we should be able to maintain 1.5 K temperature margin during continuous ramping up and down at 20 A/s (not the 36 A/s intended in the design phase). Alternatively, with a higher SHe flow rate of 16 g/s, the goal of 36 A/s should be reachable. However, we are seeing that with 10 g/s we can occasionally run at 18 A/s but occasionally we have quenches at only 10 A/s.

We conducted a parameter study to determine what might account for the low ramp rate. We could not find a credible hydraulic friction factor that would account for these low ramp rates. If we assume a thermal strain mismatch of 0.85% in the HF CICC, it reduces the temperature margin sufficiently to create quenches at 15 A/s (Fig. 2). Comparison of HF strain values is in Table IX.

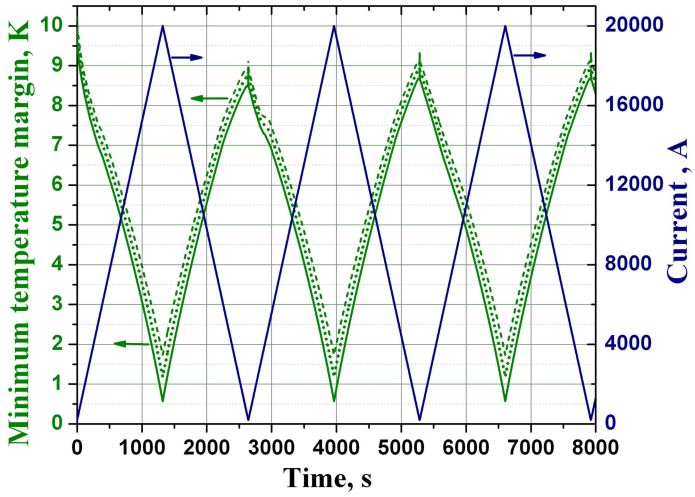

Fig. 2. Minimum temperature margin vs time for the innermost layer of the HF conductor computed at 15 A/s (0.2kA-20 kA-0.2kA cycles) and 10 g/s using the high ac loss data and different values of thermal strain mismatch: 0.65% (dash), 0.75% (dot), and 0.85% (solid lower curve).

TABLE IX
HF CICC INTERPRETATIONS

CONDUCTOR	Effective Compression (%)	I_c DEGRADATION (%)
HF CONDUCTOR TEST RESULTS	0.65	0
HF DESIGN ASSUMPTION	0.65	13
HF OPERATION	> 0.85	13

III. DISCUSSION

The fact the magnet has never reached field at 20 A/s with a 10 g/s flow rate (much less been able to operate there routinely) suggests there is more compressive strain in the Nb_3Sn than was measured in the CICC testing. However, we have not measured T_{cs} or I_c of the real CICC, so we cannot be sure.

The fact the magnet occasionally ramps without quenching at 18 A/s while it occasionally quenches while ramping at only 10 A/s is surprising. This implies something is changing in an unpredictable manner within the CICC coil.

In a CICC magnet, the SHe flows through the inside of the stainless steel conduit, in the void space between the Nb_3Sn composite wires. There is a chance that there is foreign matter in this space of the HF CICC or in the SHe inlets to the HF CICC which is being moved around by the flowing SHe and causing the flow pattern to change over time.

Fabricating a CICC coil has a number of steps. The Nb_3Sn wires are oiled during the cabling process and the inner diameter of the conduit is not cleaned after delivery. The 12 meter long pieces of conduit are butt-welded together to form pieces between 200 m and 600 m long. The cable is pulled into them and they are compacted to form the correct rectangular cross-section and internal void-space. The outer diameter of the CICC is cleaned and insulated. The coil is wound, joints are made and the coil is reacted. The glass insulation is impregnated with epoxy. Helium lines are welded onto the coil-pack and the support structure is installed. The cryostat is assembled around the cold-mass.

When one is ready to start cool-down, one starts blowing room-temperature He through the CICC. The chemical composition of the exhaust gas is checked periodically until the purity reaches an acceptable value. The coil is then deemed to be clean and cool-down begins by lowering the temperature of the incoming SHe slowly to keep the temperature variation between incoming and outgoing He < 50 K.

This process has been used to make CIC conductors and coils at a few labs. It seems unlikely that there were consistent errors at both HZB and FSU resulting in erratic performance of both magnets. Also, neither magnet has experienced problems with impurities in the He circuit impacting the refrigeration equipment.

It has also not been explained why the AC losses of real HF CICC were so much higher than those of the test CICC.

IV. Conclusion

The magnets in both Tallahassee and Berlin are running reliably, provide unique experimental capabilities worldwide, and are very popular with the solid-state NMR and neutron scattering communities, respectively.

It seems that the AC losses in CICCs can vary significantly between measurements of similar conductors and the I_c performance of Nb_3Sn CICCs is still not fully understood.

If we were planning to build another Nb_3Sn CICC coil, we would want to understand the performance of the HF CICC and would want to measure T_{cs} and I_c in leftover HF CICC from these magnets and understand the situation. But the magnets work and we have other objectives presently.

Acknowledgment

The authors would like to thank P. Smeibidl of the Helmholtz-Zentrum Berlin for providing HZB's experience operating the HZB magnet as well as the staff of Radboud University and the Swiss Plasma Center of the Ecole Polytechnique Federale de Lausanne for testing of CICCs. In addition, they are grateful to S. Hannahs for his work designing, building, and debugging the quench protection system. J. Smith has done a great job interpreting quench data and distributing it. T. Murphy has been responsible for scheduling magnet operations. M. Vanderlaan has helped with operations of the cryogenic system. The cryogenic operators and control room operators have been invaluable in debugging this system. Of course, a large team of people were involved in the design and construction of the magnet system who also played indispensable roles with great competence and enthusiasm.

References

[1] M. D. Bird, "Resistive magnet technology for hybrid inserts," *Supercond. Sci. Technol.*, vol. 17, no. 8, pp. R19–R33, 2004.

[2] M. D. Bird and Z. Gan, "Low resolution NMR magnets in the 23 to 35 T range at the NHMFL," *IEEE Trans. Appl. Supercond.*, vol. 12, no. 1, pp. 447–451, Mar. 2002.

[3] M. D. Bird *et al.*, "Commissioning of the 36 T series-connected hybrid magnet at the NHMFL," *IEEE Trans. Appl. Supercond.*, vol. 28, no. 3, 2018, Art. no. 4300706.

[4] Z. Gan *et al.*, "NMR Spectroscopy up to 35.2 T using a series-connected hybrid magnet," *J. Magn. Reson.*, vol. 284, pp. 125–136, Nov. 2017.

[5] I. R. Dixon *et al.*, "The 36-T series-connected hybrid magnet system design and integration," *IEEE Trans. Appl. Supercond.*, vol. 27, no. 4, Jun. 2017, Art. no. 4300105.

[6] P. Smeibidl *et al.*, "First hybrid magnet for neutron scattering at Helmholtz Zentrum Berlin," *IEEE Trans. Appl. Supercond.*, vol. 26, no. 4, Jun. 2016, Art. no. 4301606.

[7] A. de Ouden *et al.*, "Progress in the development of the HFML 45 T hybrid magnet," *IEEE Trans. Appl. Supercond.*, vol. 26, no. 4, Jun. 2016, Art. no. 4301807.

[8] I. R. Dixon *et al.*, "Current sharing and AC loss measurements of a cable-in-conduit conductor with Nb_3Sn strands for the high field section of the series-connected hybrid outsert coil," *IEEE Trans. Appl. Supercond.*, vol. 19, no. 3, pp. 2466–2469, Jun. 2009.

[9] I. R. Dixon, M. D. Bird, K. R. Cantrell, J. Lu, R. P. Walsh, and H. W. Weijers, "Qualification measurements of the mid-field and low-field CICC for the series-connected hybrid magnet with effects of electromagnetic load cycling and longitudinal strain," *IEEE Trans. Appl. Supercond.*, vol. 20, no. 3, pp. 1459–1462, Jun. 2010.

[10] J. Lu, H. W. Weijers, M. D. Bird, H. Ehlmer, and P. Smeibidl, "A summary of the cable-in-conduit conductor test program for the construction of the series-connected hybrid magnet," NHMFL-MST-09-OPM-560-003, Dec. 2008.

[11] N. Mitchell, "Mechanical and magnetic load effects in Nb_3Sn cable-in-conduit conductors," *Cryogenics*, vol. 43, pp. 255–270, 2003.

[12] A. V. Gavrilin, H. Bai, M. D. Bird, and I. R. Dixon, "Observations from analysis of thermohydraulic behavior of the series connected Hybrid magnets superconducting outserts," *Adv. Cryogenic Eng.*, vol. 55B, pp. 1426–1433, 2010.

[13] P. Kamil Sedlak *et al.*, "Test of the MF-CICC conductor designed for the 12-T outsert coil of the HFML 45-T Hybrid magnet," *IEEE Trans. Appl. Supercond.*, vol. 26, no. 4, Jun. 2016, Art. no. 4300305.

[14] A. Nijhuis and K. Yagotyntsev, "AC loss of HF Nb3Sn CICCs for the HFML 45 T hybrid magnet," Final Rep. UT-HFML 2015-1.v2.0., 2015.